Dilatancy, failure, and fluid flow in basalt: Implications for geothermal reservoirs

Patrick Baud[1], Wei Zhu[2], Jamie Farquharson[1], Teng-fong Wong[3], Michael Heap[1], Sergio Vinciguerra[4]

[1] University of Strasbourg, EOST, IPGS, UMR 7516 CNRS, 5 rue René Descartes; 67084, Strasbourg France

[2] Department of Geosciences, State University of New York, Stony Brook, New York, USA

[3] Earth System Science Programme, Faculty of Science, The Chinese University of Hong Kong, Hong Kong

[4] Department of Earth Sciences, University of Turin, Italy

patrick.baud@unistra.fr

Keywords: volcanic rocks, microcracks, damage, porosity.

ABSTRACT

Understanding how the strength of volcanic rocks varies with stress state, pressure and microstructural attributes is fundamental to understanding the dynamics of geothermal reservoirs. In this study we investigated the micromechanics of deformation and failure in basalts. We performed uniaxial and triaxial compression experiments samples covering a porosity range between 5 and 16%, at effective pressures up to 200 MPa. Dilatancy and brittle faulting were observed in all samples with porosity of 5%. Shear-enhanced compaction was observed at effective pressures as low as 80 MPa in samples of 8% porosity and more. Microstructural data revealed the complex interplay of microcracks and pores on dilatant failure and inelastic compaction in basalt. The micromechanics of brittle failure was controlled by wing crack propagation under triaxial compression in low porosity end members, and by pore-emanated cracking in the more porous samples. Permeability of basalt was found less sensitive to porosity then mechanical strength.

1. INTRODUCTION

A systematic investigation of basalt deformation and failure mode is of fundamental importance for the understanding of basaltic geothermal systems [Ásmundsson et al. 2014; Fowler et al; 2015; Pope et al. 2015]. Numerous studies have been conducted on the elastic and transport properties of basalts and how they evolve with hydrostatic loading (Vinciguerra et al. 2005; Fortin et al. 2010). There have also been investigations of brittle failure and creep of relatively low-porosity basalts (e.g., Rocchi et al; 2004; Benson et al. 2007; Heap et al. 2011; Violay et al. 2015). Recent studies (Loaiza et al. 2012, Adelinet et al. 2013), showed that the phenomenology of failure in porous basalt is qualitatively similar to that in porous siliciclastic and carbonate rocks (Wong and Baud, 2012).

Because most of the previous rock mechanics studies of basalt are site specific and consider samples of a relatively narrow range of porosity, questions on how porosity and preexisting damage influence failure remain unresolved. To fill the gap, we performed compression experiments on several blocks of basalt samples from Mount Etna, with porosities ranging from 5% to 16.0% and on a block of Reykjanes basalt from Iceland of 11% porosity. We then studied the micromechanics of brittle faulting and shear-enhanced compaction in these rocks based on systematic microstructural observations of deformed samples, in order to analyze the development of inelastic damage and failure that could occur in a geothermal system.

2. MATERIAL STUDIED

Our blocks of Etna basalt were acquired from a quarry at the same location described by Heap et al. (2009). As one of eight major rock types categorized by Tanguy et al. (1997), this basalt is a porphyritic alkali basalt considered to be the most representative basalt from the volcano. It is made of mm-sized phenocrystals of pyroxene, olivine and feldspar in a fine-grained groundmass. Our samples covered a porosity range between 5 and 16%. Microstructural observations of the intact material revealed the presence of thin cracks and variable concentrations of quasi-spherical pores of various sizes. We also studied a few samples of Reykjanes basalt from Iceland, taken from the same block previously studied by Adelinet et al. (2013), who provided a detailed description of this rock. The average porosity of our samples of Reykjanes basalt was found to be 11.2%.

3. EXPERIMENTAL PROCEDURE

Uniaxial compression strength (UCS) tests were conducted in Strasbourg. Details on the experimental set-up can be found in Heap et al. (2014). Triaxial compression experiments were performed at the Stony Brook laboratory on water-saturated samples. The two laboratories followed similar sample preparation and experimental protocols. For wet experiments, the samples were first dried in vacuum at 80°C for several days and then saturated with distilled water. The jacketed samples were then deformed in conventional

triaxial configuration at room temperature and at a strain rate of 10^{-5}/s. Samples saturated with deionized water were deformed with the pore pressure maintained at 10 MPa under fully drained conditions (see Zhu et al. 2011 for details).

Permeability was measured in Strasbourg on a selection of intact samples, at a confining pressure of 1 MPa using the protocol described by Farquharson et al. (2015).

4. MECHANICAL DATA

We found that the UCS of dry Etna basalt varied by more than a factor 5 in the porosity range 5-14% (Figure 1). More variability was also observed for the low porosity end-members. This large range and variability is mostly due to the different concentrations and sizes of vesicles in this basalt.

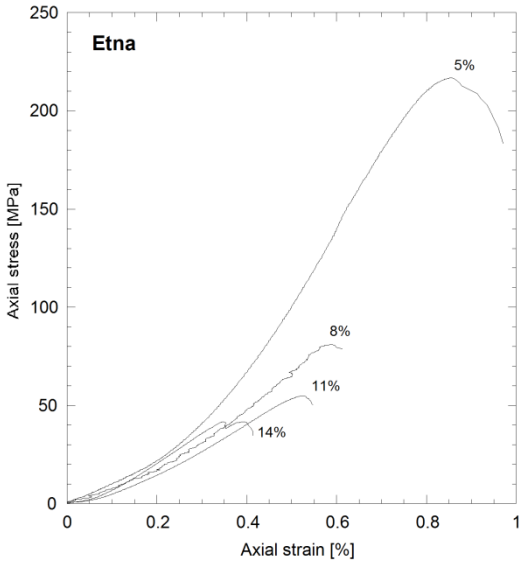

Figure 1: Uniaxial compression data on sample of Etna basalt of different porosities. Axial stress is presented as a function of axial strain.

Overall the mechanical responses of wet samples of 5% porosity at effective pressures ranging from 10 MPa to 150 MPa were qualitatively similar (Figure 2). The differential stress of a sample first attained a peak, beyond which strain softening was observed and the differential stress dropped to a residual level. Except for two samples deformed at the highest effective pressure of 150 MPa, instability with dynamic stress drop was observed in the post-failure stage of each sample. Dilatancy was recorded pre-peak in all experiments. The onset of dilatancy was followed by a sharp increase in acoustic emission activity, as observed in other rock types. This failure mode is typical of the brittle faulting regime. Post-mortem visual inspection of the samples revealed the development of shear band oriented at various angles to the direction of the major principal stress.

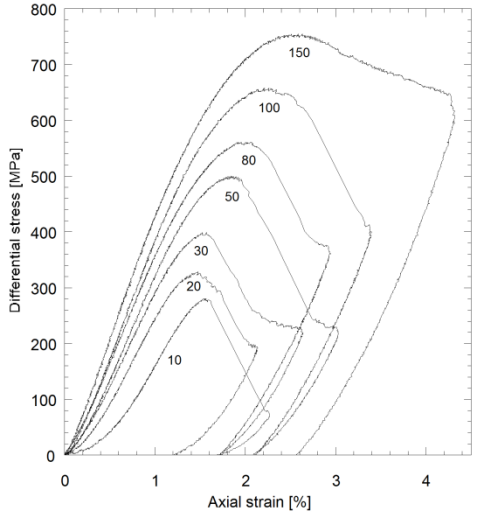

Figure 2: Mechanical data for wet experiments on Etna basalt. Differential stress is plotted versus axial strain. Numbers next to each curve indicate the effective pressure maintained during the experiment

The tangent modulus was derived from the slope of the stress-strain curves in the elastic part of the curves presented in Figure 2. There is a trend for this modulus to increase with effective pressure in an approximately linear manner (Figure 3). The progressive closure of the microcracks made Etna basalt significantly stiffer at high effective pressures.

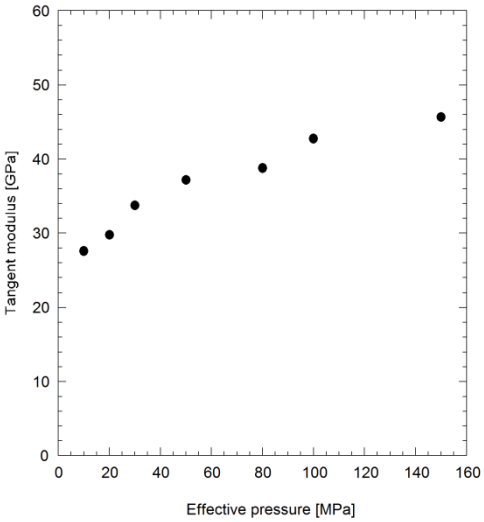

Figure 3: Tangent modulus as a function of effective pressure for samples of Etna basalt of 5% porosity.

We fit the data (Figure 4) using the Hoek-Brown criterion

$$\sigma_1 = \sigma_3 + \sqrt{m\sigma_c\sigma_3 + \sigma_c^2} \quad [1]$$

where m is constant and σ_c is uniaxial strength. For Mount Etna's basalt we obtained σ_c =224 MPa and m = 16. In two recent studies the Hoek-Brown's relation was used by Okubo (2004) and Moon et al. (2005) in their assessment of the stability of the Hilina slump, Kilauea volcano and stratocone crater wall sequences,

White Island volcano, New Zealand. In the absence of triaxial experiment data on basalt, their choices of the strength parameters were relatively unconstrained. Our data can now provide useful constraints on such analyses.

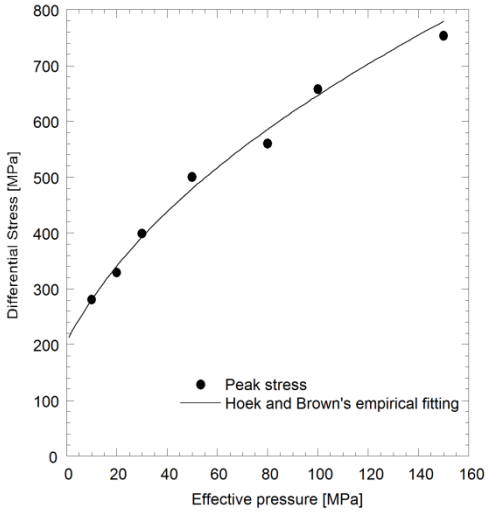

Figure 4: Peak stresses (symbols) for samples of Etna basalt that failed in the brittle manner are plotted as a function of effective pressure. An empirical fit using Hoek and Brown's relation is also shown as a solid line.

Beyond a porosity of 10%, vesicle size (diameter of 0.5 cm and greater) in Etna basalt made it difficult to perform triaxial experiments. We therefore studied the mechanical behaviour of Reykjanes basalt, with 11.2% porosity and smaller vesicle sizes. We focussed on high effective pressures since Adelinet et al. (2013) previously studied the mechanical behaviour of this rock in the 0-100 MPa range. Figure 5 presents the mechanical for two experiments performed at 140 and 200 MPa.

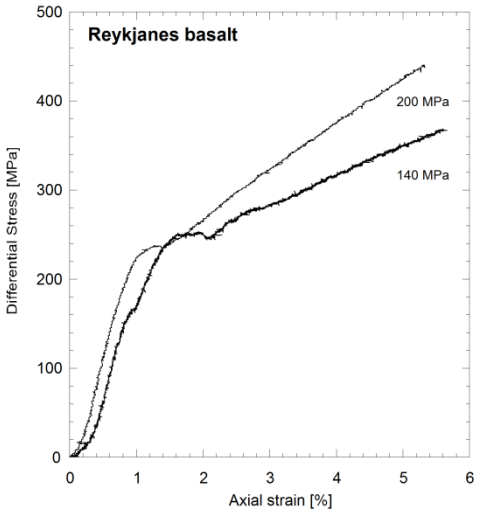

Figure 5: Mechanical data for Reykjanes basalt (Iceland). Differential stress is plotted as a function of axial strain for two experiments performed at 140 and 200 MPa of effective pressures.

These data are typical of a ductile behaviour with no peak stress and significant strain hardening. Figure 6 also shows that significant inelastic compaction (shear-enhanced compaction) could occur in porous basalt under relatively high effective pressures. Adelinet et al. (2013) also revealed the development of compaction localization in Reykjanes basalt in this regime.

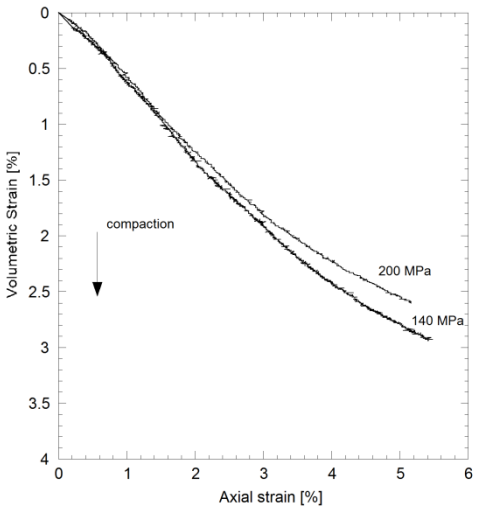

Figure 6: Peak stresses (symbols) for samples of Etna basalt that failed in the brittle manner are plotted as a function of effective pressure. An empirical fit using Hoek and Brown's relation is also shown as a solid line.

5. MICROSTRUCTURAL ANALYSIS

Microstructure of triaxially deformed samples compressed to different stages of deformation and then carefully unloaded, was studied using a scanning electron microscopes (SEM) on polished thin-sections.

For samples of Etna basalt deformed in the brittle faulting regime, our microstructural analysis revealed two mechanisms of stress-induced damage. We first observed stress-induced cracking that has developed primarily by the reopening of sealed cracks, preferentially aligned with the direction of the major principal stress (Figure 7).

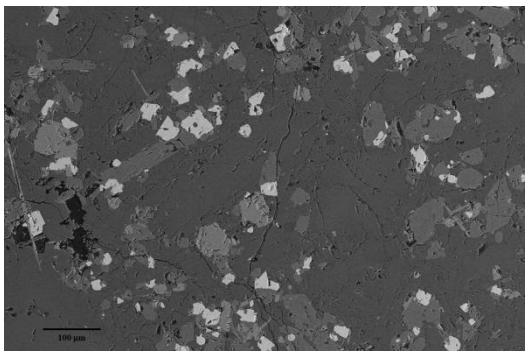

Figure 7: Backscatter SEM image of a sample of Etna basalt of 5% porosity deformed at an effective pressure of 10 MPa beyond the peak stress. The direction of the major principal stress was vertical.

We also observed pore-emanated microcracks pre- and post-peak in most of our samples (Figure 8). Our systematic microstructural analysis suggested that this second mechanism was pronounced in samples with porosity >8%.

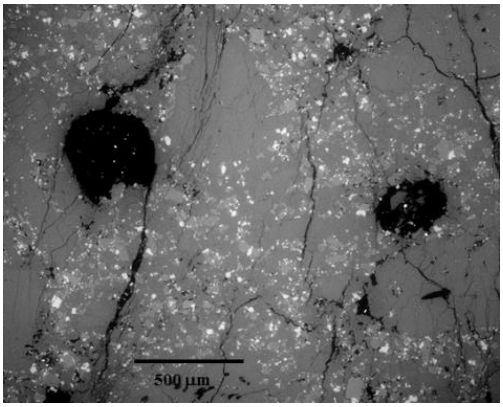

Figure 8: Backscatter SEM image of a sample of Etna basalt of 8% porosity deformed at an effective pressure of 80 MPa up to the peak stress. The direction of the major principal stress was vertical.

Our observations on Reykjanes basalt samples deformed at high effective pressures revealed that cataclastic pore collapse was the main mechanism of inelastic compaction in this rock as it was previously observed in limestone (Vajdova et al. 2012) and tuff (Zhu et al. 2011).

6. MICROMECHANICAL MODELING

In low porosity basalt, our microstructural observations indicate that the micromechanics of brittle failure is dominated by wing crack growth related to the preexisting cracks, with pore-emanated cracking playing a secondary role. A micromechanical model that has been used extensively to describe processes akin to our microstructural observations in triaxially compressed basalt samples is the sliding wing crack model (Ashby and Sammis 1990). The model considers sources of tensile stress concentration that are located at the tips of preexisting cracks (of length 2c). The applied far-field stresses induce a shear traction on the crack plane, and if the resolved shear traction exceeds the frictional resistance (characterized by the friction coefficient μ) along the closed crack, frictional slip occurs which also induces tensile stress concentrations at the two tips that may nucleate and propagate wing cracks parallel to the vertical direction. As wing cracks grow to longer distances, they interact and ultimately coalesce to result in an instability. At the peak stress, the sliding wing crack model predicts that the principal stresses would also fall on a linear trend, with slope and intercept related to the crack length, friction coefficient and fracture toughness K_{IC}, as well as an additional non dimensional parameter D_0 that characterizes the "initial damage" (or "crack density").

We fitted the data presented in Figure 2 (for Etna basalt of 5% porosity) using the model of Ashby and Sammis (1990), and following the procedure detailed in Baud et al. (2014), found the following values for the model parameters: D_0 = 0.14, μ=0.5 and $K_{IC}/(\pi c)^{1/2}$ = 82 MPa. According to experimental measurements on common silicate minerals, the value of K_{IC} is ~0.3 MPa $m^{1/2}$ for feldspars, and can be higher in other silicate minerals such as quartz and olivine. However, if the induced cracking develops along a sealed crack, K_{IC} is expected to be lower, possibly by a factor of 2 or so (Atkinson and Meredith, 1987). If we assume K_{IC} = 0.3 MPa $m^{1/2}$, the predicted preexisting microcrack length is in the range 10-100 µm, in qualitative agreement with our microstructural observations.

We used the inferred parameters to predict the UCS of Etna basalt over the whole porosity range. If consistent results were obtained for porosity <8%, we found that beyond this limit the wing crack model significantly overestimated the strength of Etna basalt. This is not unexpected since our microstructural observations revealed that pore-emanated microcracking could also contribute to a significant part of the macroscopic inelastic strain. Sammis and Ashby (1986) proposed a 2-dimensional damage mechanics model that considers an elastic medium pervaded by circular holes of uniform radius r. As the applied stress increases, a point is reached when the stress intensity factor of a small crack on the circular surface attains the critical value K_{IC}, at which point extensile cracks would initiate from the poles and propagate in to a certain distance in the direction of major principal stress. As the stress-induced cracks propagate to longer distances with increasing stress, they interact with one another to induce additional tensile stress intensity, ultimately leading to an instability with coalescence of the pore-emanated cracks at the peak stress level. At a fixed lateral stress, Sammis and Ashby's (1986) pore-emanated cracking model predicts that the peak differential stress scales with the parameter. For uniaxial compression, Zhu et al. (2010) obtained an analytic estimate of the UCS, as a function of porosity φ:

$$UCS = \frac{1.325}{\varphi^{0.414}} \frac{K_{IC}}{\sqrt{\pi r}} \qquad [2]$$

The model therefore predicts a one-to-one correspondence between UCS and porosity for rocks with similar pore sizes. Figure 9 shows how UCS would evolve with porosity according to the model for different pore sizes. For our more porous Etna basalt samples, the UCS is consistent (see Figure 1) with a pore diameter of about 1.1 cm, comparable to few very large pores visible on the sample surface. Figure 9 therefore suggests that for the high porosity end members, the strength of basalt is mostly controlled by the vesicle size. In the intermediate porosity range, the contribution of both wing cracks and pore-emanated microcracks should be considered to model brittle failure of basalt.

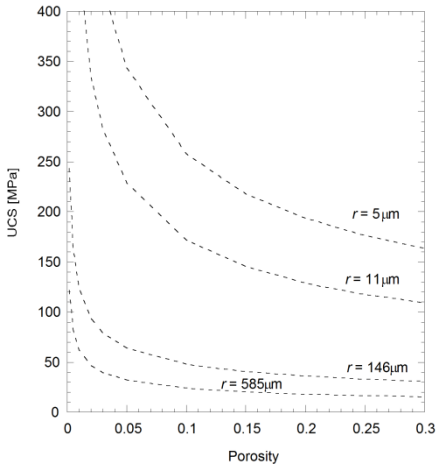

Figure 9: Predictions of Equation 2 assuming K_{IC} = 0.3 MPa m$^{1/2}$. UCS is plotted as a function of porosity.

7. PERMEABILITY

The permeability of intact samples of Etna and Reykjanes basalts was also measured at low confining pressure using gas. For Etna basalt, we found a permeability in the range 5×10^{-17} to 9×10^{-16} m^2 (for porosity between 4 and 15%), which is in general agreement with previous measurements of Fortin et al. (2010). The higher permeability was obtained for the most porous samples of porosity ~15%. For Reykjanes basalt, we somehow obtained a comparable range, 8×10^{-16} to 1.2×10^{-14}, but for a much smaller porosity interval of 10.4 to 11.6%. That is less than 1%. Taken together these new data show clearly that, because the vesicles are connected by microcracks, they do not have a major impact on fluid flow. This means in turn that it is the crack density rather than the volume of vesicles that could be considered as an important parameter controlling fluid flow in basalt. Stress-induced microcracking, as observed in our deformed samples, is therefore likely to have a significant impact on permeability of basalt.

8. CONCLUSIONS

We investigated the micromechanics of deformation and failure in basalt, focusing on core samples from Mt Etna. Our observations on undeformed samples of porosity ranging from 4 to 16% show the complex microstructure of these volcanic rocks, with pores of various sizes, microcracks and different proportions of phenocrysts. Dilatancy and brittle faulting were observed in all deformed samples under relatively low effective pressures. While stress-induced cracking was observed to develop primarily by the reopening of sealed cracks in the low porosity end-members, pore-emanated microcracking becomes the dominant mechanism of stress-induced damage leading to brittle faulting in the more porous basalts. At relatively high effective pressures, our new data confirmed that inelastic compaction could occur in porous basalt, due to homogeneous or localized cataclastic pore collapse. Our full set of data could be found in Zhu et al. (in review).

Our study suggested that in a basaltic geothermal environment, very large differences in mechanical parameters (elastic moduli, strength) are to be expected, mostly because of the density and size of vesicles and microcracks. For high porosities, the strength of basalt is to the first order controlled by the vesicle size. In contrast, these voids, which contribute to the major part of the porosity, do not induce significant variations of the permeability, essentially because they are always connected by microcracks.

Hydro-mechanical modeling in geothermal sites should therefore take into account the geometric attributes of porosity for the mechanical part and the impact of stress-induced damage on fluid flow.

REFERENCES

Adelinet, M., Fortin, J., Schubnel, A. and Guéguen, Y.: Deformation modes in Icelandic basalt: From brittle failure to localized deformation bands, *J. Vol. Geoth. Res*., **255**, (2013), 15-25.

Ashby, M. F. and Sammis, C. G.: The damage mechanics of brittle solids in compression, *Pure Appl. Geophys.*, **133**, (1990), 489-521.

Atkinson, B. K., and Meredith, P. G.: Experimental fracture mechanics data for rocks and minerals, in *Fracture Mechanics of Rock*, edited by B. K. Atkinson, pp. 477-525, Academic Press, London (1987).

Baud, P., Wong, T.-f., and Zhu, W.: Effects of Porosity and Crack Density on Compressive Strength of Rocks, *Int. J. Rock Mech. Min. Sci*., **67**, (2014), 202-211.

Benson, P. M., Thompson, B. D., Meredith, P. G., Vinciguerra, S., Young, R. P.:, Imaging slow failure in triaxially deformed Etna basalt using 3D acoustic-emission location and X-ray computed tomography, *Geophys. Res. Lett.*, **34**, (2007).

Farquharson, J. I., Heap, M. J., Varley, N., Baud, P. and Reuschlé, T.: Permeability and porosity relationships of edifice-forming andesites: A combined field and laboratory study, Journal of Volcanology and Geothermal Research, **297**, (2015), 52-68.

Fortin, J., Stanchits, S., Vinciguerra, S., and Guéguen, Y.: Influence of thermal and mechanical cracks on permeability and elastic wave velocities in a basalt from Mt. Etna volcano subjected to elevate pressure, *Tectonophysics*, **503**, (2010), 60–74.

Fowler, A. P. G., Zierenberg, R. A., Schiffman, P., Marks, N., and Friõleifsson, G. O.: Evolution of fluid–rock interaction in the Reykjanes geothermal system, Iceland: Evidence from Iceland Deep Drilling Project core RN-17B, *J. Vol. Geotherm. Res*., **302**, (2015), 47-63.

Heap, M. J., Vinciguerra, S. and Meredith, P. G., The evolution of elastic moduli with increasing crack damage during cyclic stressing of a basalt from

Mt. Etna volcano, *Tectonophysics*, *471*(1-2), (2009), 153-160.

Heap M. J. , Baud P., Meredith P. G., Vinciguerra S.**,** Bell A. F. and Main I. G.: Brittle creep in basalt from Mt Etna volcano: implications for time-dependent volcano deformation, *EPSL*, (2011).

Heap, M. J., Petrakova, L., Lavallée, Y., Baud, P., Varley, N. R. and Dingwell D. B.: Microstructural controls on the physical and mechanical properties of edifice-forming andesites at Volcan de Colima, Mexico, *J. Geophys. Res*., **119**, (2014).

Loaiza, S., Fortin, J., Schubnel, A., Guéguen, Y., Vinciguerra, S. and Moreira, M.: Mechanical behavior and localized failure modes in a porous basalt from the Azores, *Geophys. Res. Lett*., **39**, (2012).

Moon, V., Bradshaw, J., Smith, R. and de Lange, W.: Geotechnical characterization of stratocone crater wall sequences, White Island Volcano, New Zealand, *Eng. Geol*., **81**, (2005), 146-147.

Okubo, C. H.: Rock mass strength and slope stability of the Hilina slump, Kilauea volcano, Hawaii, J. of Volcano. *Geotherm. Res*., **138**, (2004), 43-76.

Pope, E. C., Bird, D. K., Arnorsson, S. and Giroud N.: Hydrogeology of the Krafla geothermal system, northeast Iceland, *Geofluids*, **16 (1)**, (2015), 175-197.

Rocchi, V., Sammonds, P. R. and Meredith, P. G.: Fracturing Etnean and Vesuvian rocks at high temperature and low pressures, *J. Vol. Geoth Res*., **132,** (2004), 137-157.

Sammis, C. G. and Ashby, M. F.: The failure of brittle porous solids under compressive stress states, *Acta metall*., **34**, (1986), 511-526.

Tanguy J. C., Condomines, M. and Kieffer, G.: Evolution of Mount Etna magma: constraints on the present feeding system and eruptive mechanism, *J. Volcan. Geoth. Res*., **75**, (1997), 221–250.

Vajdova, V., Baud, P., Wu, L. and Wong, T.-f.: Micromechanics of inelastic compaction in two allochemical limestones, *J. Struct. Geol*., 43, (2012), 100-117.

Vinciguerra, S., Trovato, C., Meredith, P. G. and Benson, P.: Relating seismic velocities, thermal cracking and permeability in Mt. Etna and Iceland basalts, *Int J Rock Mech Min*, **42**, (2005), 900-910.

Violay, M., Gibert, B., Mainprice, D. and Burg, J.-P: Brittle versus ductile deformation as the main control of deep fluid circulation in oceanic crust, *Geophys. Res. Lett.*, **42 (8)**, (2015), 2767-2773.

Wong, T.-f. and Baud, P.: The brittle-ductile transition in rocks: A review, *J. Struct. Geol*., **44**, (2012), 25-53.

Zhu, W., Baud, P., Vinciguerra, S. and Wong, T.-f.: Micromechanics of brittle faulting and cataclastic flow in Alban Hills Tuff, *J. Geophys. Res*., **106**, (2011).

Zhu, W., Baud, P., Vinciguerra, S. and Wong, T.-f.: Micromechanics of brittle faulting and cataclastic flow in Mt Etna basalt, *J. Geophys. Res*., in review.

Acknowledgements

The research at Strasbourg and Hong Kong were partially funded by the France-Hong-Kong Collaborative Program Procore 30805PM and F-CUHK406/13, respectively. This work was also partially funded by the LABEX G-EAU-THERMIE profonde of the University of Strasbourg.